

Fig. S1. XPS spectrum of pure La_2O_3 .

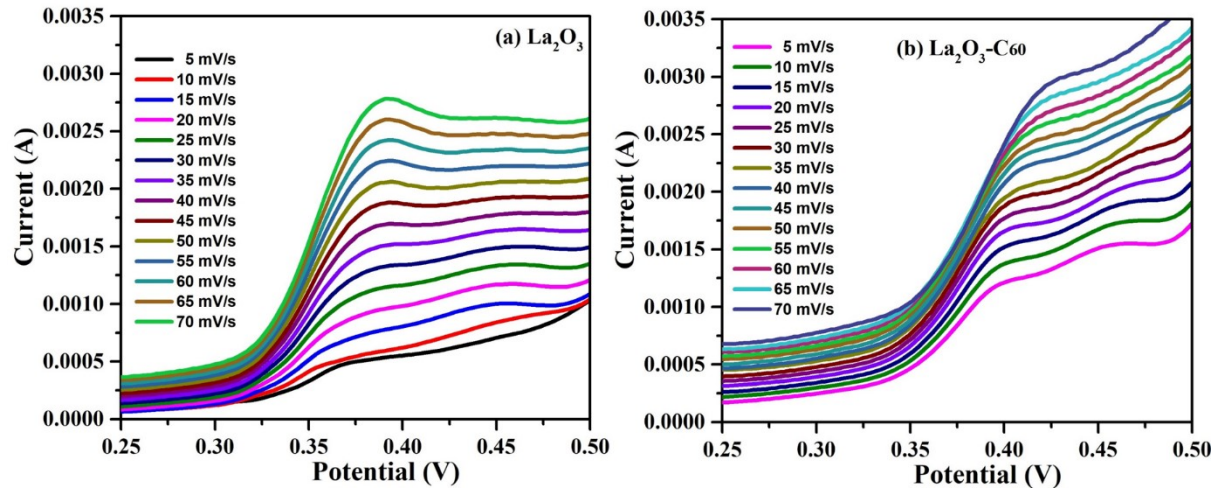


Fig. S2. Linear sweep voltammetry (LSV) curves at varying scan rates (a) pure La_2O_3 (b) $\text{La}_2\text{O}_3\text{-C}_60$ nanocomposite.

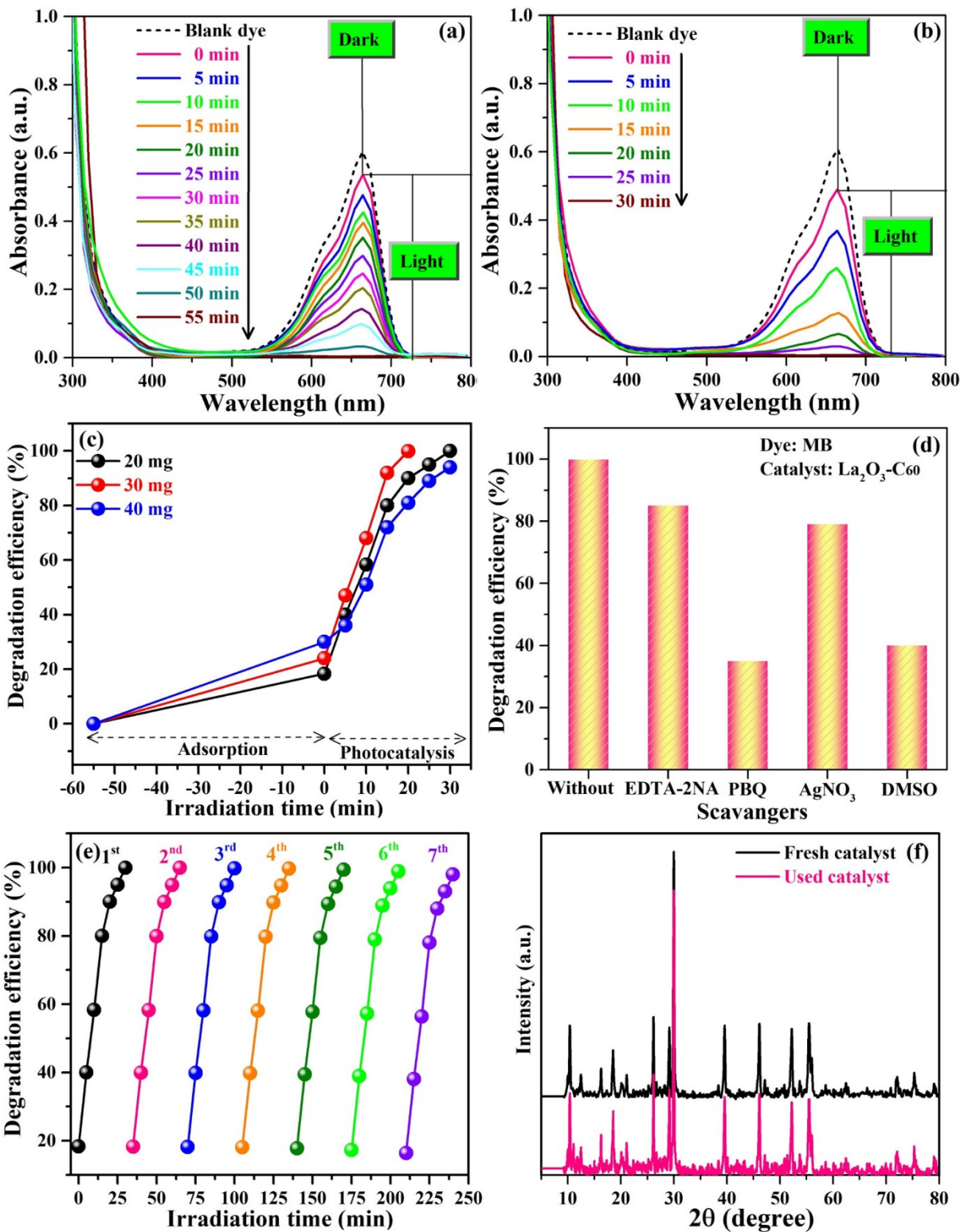


Fig. S3. absorption spectra of MB solution under UV-light irradiation at different times, (a) La₂O₃, (b) La₂O₃-C₆₀ nanocomposite (c) degradation efficiency at varying catalyst amount, (d) photodegradation by adding different scavengers, (e) reusability profile, and (f) XRD pattern of the fresh and used catalyst after recyclability test.

Table S1. Comparison of specific capacitance of grown La_2O_3 - C_{60} nanocomposites with other reported electrode materials.

Material	Electrolytes	Specific Capacitance (Fg^{-1})	Scan rate (mVs^{-1})	Ref.
La_2O_3 -rGO	1 M H_2SO_4	692	10	¹
La_2O_3 // Co_3O_4	1 M KOH	15	5	²
Zn doped CdO	6M KOH	388	10	³
CdO	NaOH	267	5	⁴
La_2O_3 thin film	1 M KOH	147	5	⁵
ZnO /rGO	1 M Na_2SO_4	95	10	⁶
La_2O_3	1M KOH	250	5	⁷
Cr_2O_3 -carbon	6 mol/L KOH	300	2	⁸
Cr_2O_3 /rGO	2M KOH	206	10	⁹
La_2O_3	1M LiClO_4	166	5	¹⁰
Ag- La_2O_3	0.1 M NaOH	33	5	¹¹
Cr doped NiO	3M KOH	636	5	¹²
La_2O_3-C_{60}	1M KOH	741	5	Present

Table S2. Photo-degradation kinetics parameters for La₂O₃ and La₂O₃-C₆₀ nanocomposites.

Equation: y = a + b*x						
Catalysts	Intercept	Slope = K (min ⁻¹)	Adj. R-Square	Pearson's r	Residual Sum of Squares	
La ₂ O ₃	-0.19333	0.04681	0.80771	0.90936	1.26082	
C ₆₀	0.25526	0.02206	0.87618	0.94264	0.1678	
La ₂ O ₃ -C ₆₀	-0.01785	0.11472	0.96916	0.98759	0.14566	

References

- 1 M. Miah, S. Bhattacharya, D. Dinda and S. K. Saha, Temperature dependent supercapacitive performance in La₂O₃ nano sheet decorated reduce graphene oxide, *Electrochim. Acta*, 2018, **260**, 449–458.
- 2 A. A. Yadav, A. C. Lokhande, J. H. Kim and C. D. Lokhande, High electrochemical performance asymmetric supercapacitor based on La₂O₃//Co₃O₄ electrodes, *J. Ind. Eng. Chem.*, 2017, **56**, 90–98.
- 3 M. I. Pratheepa and M. Lawrence, Synthesis of pure, Cu and Zn doped CdO nanoparticles by co-precipitation method for supercapacitor applications, *Vacuum*, 2019, **162**, 208–213.
- 4 S. Patil, S. Raut, R. Gore and B. Sankapal, One-dimensional cadmium hydroxide nanowires towards electrochemical supercapacitor, *New J. Chem.*, 2015, **39**, 9124–9131.
- 5 A. A. Yadav, V. S. Kumbhar, S. J. Patil, N. R. Chodankar and C. D. Lokhande, Supercapacitive properties of chemically deposited La₂O₃ thin film, *Ceram. Int.*, 2016, **42**, 2079–2084.
- 6 T. Prabhuraj, S. Prabhu, E. Dhandapani, N. Duraisamy, R. Ramesh, K. A. R. Kumar and P. Maadeswaran, Bifunctional ZnO sphere/r-GO composites for supercapacitor and photocatalytic activity of organic dye degradation, *Diam. Relat. Mater.*, 2021, **120**, 1–9.
- 7 A. A. Yadav, A. C. Lokhande, J. H. Kim and C. D. Lokhande, Supercapacitive activities of porous La₂O₃ symmetric flexible solid-state device by hydrothermal method, *Int. J. Hydrogen Energy*, 2016, **41**, 18311–18319.
- 8 S. Ullah, I. A. Khan, M. Choucair, A. Badshah, I. Khan and M. A. Nadeem, A novel Cr₂O₃-carbon composite as a high performance pseudo-capacitor electrode material, *Electrochim. Acta*, 2015, **171**, 142–149.

- 9 C. Song, Y. Gui, X. Xing and W. Zhang, Well-dispersed chromium oxide decorated reduced graphene oxide hybrids and application in energy storage, *Mater. Chem. Phys.*, 2016, **173**, 460–466.
- 10 J. Zhang, Z. Zhang, Y. Jiao, H. Yang, Y. Li, J. Zhang and P. Gao, The graphene/lanthanum oxide nanocomposites as electrode materials of supercapacitors, *J. Power Sources*, 2019, **419**, 99–105.
- 11 H. Wang, X. Yan and G. Piao, A high-performance supercapacitor based on fullerene C60 whisker and polyaniline emeraldine base composite, *Electrochim. Acta*, 2017, **231**, 264–271.
- 12 R. Ahmed and G. Nabi, Enhanced Electrochemical Performance of Cr-doped NiO Nanorods for Supercapacitor Application, *J. Energy Storage*, 2021, **33**, 102115.